6th European Conference on Computational Mechanics (ECCM 6)
7th European Conference on Computational Fluid Dynamics (ECFD 7)
11-15 June 2018, Glasgow, UK

CLASSICAL SHELL ANALYSIS IN VIEW OF TANGENTIAL DIFFERENTIAL CALCULUS

Daniel Schöllhammer[1], **Thomas-Peter Fries**[2]

[1,2] Institute of Structural Analysis, Graz University of Technology, Lessingstr. 25/II, 8010 Graz, Austria, www.ifb.tugraz.at,

[1] schoellhammer@tugraz.at, [2] fries@tugraz.at

Key words: Shells, Tangential Differential Calculus, TDC

Abstract. We propose a reformulation of the classical Kirchhoff-Love shell equations in terms of tangential differential calculus, which is independent of a parametrization of the middle surface. An advantage of our approach is that the surface may be defined implicitly, and the resulting shell equations and stress resultants lead to a more compact and intuitive implementation. Numerical tests are performed and it is confirmed that the obtained approach is equivalent to the classical formulation based on local coordinates.

1 INTRODUCTION

In the classical approach of modelling shells, the middle surface is defined by a parametrization. Based on this parametrization a local coordinate system with co- and contra-variant base vectors is introduced, and for curved shells the well-known Christoffel symbols naturally occur, which makes the approach less intuitive and more complex. An overview in classical shell theory is given in e.g. [20, 21, 6, 1, 24, 3].

A first approach, which does not need a parametrization of the middle surface, is introduced by Delfour and Zolésio [7, 8]. They define the shell implicitly via signed distance functions and the surface derivatives are defined in terms of the tangential differential calculus (TDC). For instance, in [18, 22] this approach is already used to model thin shells; membranes are considered in [12, 14]. A recent approach, which is limited to thin, flat shells embedded in $\mathbb{R}^3$ is given in [13]. An advantage of this approach based on TDC is that the resulting boundary value problem (BVP) can be discretized with new finite element techniques such as TraceFEM [19] or CutFEM [4, 5], where a parametrization is not available.

The governing equations in these works are rather technical and focus on the mathematical background. Herein, the focus is on a compact and intuitive formulation, the definition of mechanical quantities, and the implementation. Stress resultants such as normal forces and bending moments are defined in a global Cartesian coordinate system. The equilibrium of the shell in strong form is expressed in terms of the stress resultants and leads to a 4^{th} order boundary value problem (BVP). The BVP is discretized with the surface FEM [11] using NURBS as trial and test functions due to the continuity requirements of Kirchhoff-Love shells.

The outline of the paper is as follows. In Section 2, important surface quantities are defined, and an introduction to the tangential differential calculus is given. In Section 3, the classical linear Kirchhoff-Love shell equations under static loading are recast in terms of tangential differential calculus. The stress resultants are defined and compared to the well-known expressions in the classical theory. In Section 4, implementational aspects are considered and the element stiffness matrix and the resulting system of linear equations are shown. Finally, in Section 5, the shell obstacle course proposed by Belytschko et al. [2] is performed.

2 PRELIMINARIES

A shell is a geometrical object, which is in one dimension significantly smaller compared to the other directions. In other words, the 3D-shell continuum can be described by its middle surface Γ. The middle surface is embedded in the physical space $\mathbb{R}^3$ as illustrated in Figure 1. In general, the surface may be described explicitly with a map $\boldsymbol{x}(\boldsymbol{r}) : \mathbb{R}^2 \to \mathbb{R}^3$ (see Figure 1a) or implicitly (see Figure 1b), i.e. with level-set functions. In both descriptions, there exists a unit outward normal vector $\boldsymbol{n}_\Gamma \in \mathbb{R}^3$, a tangential vector $\boldsymbol{t}_{\partial\Gamma}$, which is at the boundary $\partial\Gamma$ and a co-normal vector $\boldsymbol{n}_{\partial\Gamma}$, which is perpendicular to $\boldsymbol{n}_\Gamma$ and $\boldsymbol{t}_{\partial\Gamma}$ pointing „outwards“ of the middle surface in tangential direction.

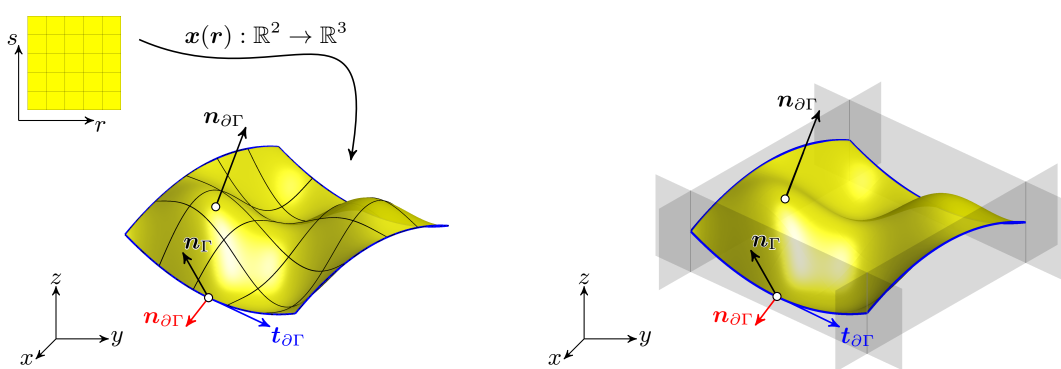

(a) Explicit surface description with the map $\boldsymbol{x}(\boldsymbol{r})$

(b) Implicitly defined surface with a master level-function $\phi(\boldsymbol{x}) = 0$ (yellow) and slave level-set functions ψ_i for the boundary definition (gray)

Figure 1: Examples of explicitly and implicitly definition of middle surfaces

2.1 Tangential differential calculus

In tangential differential calculus (TDC), surface derivatives can be defined in terms of a Cartesian coordinate system. In the following, the surface gradients and surface divergence operators are briefly defined. A more detailed introduction to TDC is given in [9].

The orthogonal projection operator or normal projector $\mathbf{P}$, which projects vectors to the tangent space $T_P\Gamma$ of the manifold, is defined as

$$\mathbf{P} = \mathbb{I} - \boldsymbol{n}_\Gamma \otimes \boldsymbol{n}_\Gamma \ . \tag{1}$$

Let us consider a scalar function $f(\boldsymbol{x}_\Gamma) : \Gamma \to \mathbb{R}$. A smooth extension of f in the neighbourhood $\mathcal{U}$ of the surface Γ can be achieved by a closest point projection $\boldsymbol{\eta}(\boldsymbol{x}) : \mathcal{U} \to \Gamma$, i.e. $\tilde{f} = f \circ \boldsymbol{\eta}$. Alternatively, the function $\tilde{f}(\boldsymbol{x})$ may also be defined in the physical space $\mathbb{R}^3$ and is then restricted to the manifold Γ. In this case, we introduce the surface gradient operator ∇_Γ for scalar valued functions

$$\nabla_\Gamma f(\boldsymbol{x}_\Gamma) = \mathbf{P}(\boldsymbol{x}_\Gamma) \cdot \nabla \tilde{f}(\boldsymbol{x}_\Gamma) \ . \tag{2}$$

For parametrized manifolds with the map $\boldsymbol{x}(\boldsymbol{r}) : \mathbb{R}^2 \to \mathbb{R}^3$ and a given scalar function defined in the reference space $f(\boldsymbol{r}) : \mathbb{R}^2 \to \mathbb{R}$, the surface gradient can be expressed in terms of the Jacobi-matrix $\mathbf{J} = \frac{\partial \boldsymbol{x}}{\partial \boldsymbol{r}}$ and the gradient in the reference space $\nabla_{\boldsymbol{r}}$

$$\nabla_\Gamma f = \mathbf{J} \cdot (\mathbf{J}^\intercal \cdot \mathbf{J})^{-1} \cdot \nabla_{\boldsymbol{r}} f \ . \tag{3}$$

The components of $\nabla_\Gamma f$ are denoted as $\partial^\Gamma_{x_i} f$ or $f_{,i}$ with $i = 1, 2, 3$. The directional surface gradient $\nabla^{\text{dir}}_\Gamma$ for vector valued functions $\boldsymbol{v}(\boldsymbol{x}_\Gamma) : \Gamma \to \mathbb{R}^3$ is defined as the application of the surface gradient for scalars to the components of the vector $\boldsymbol{v}$

$$\nabla^{\text{dir}}_\Gamma \boldsymbol{v}(\boldsymbol{x}_\Gamma) = \begin{bmatrix} \nabla_\Gamma u^\intercal(\boldsymbol{x}_\Gamma) \\ \nabla_\Gamma v^\intercal(\boldsymbol{x}_\Gamma) \\ \nabla_\Gamma w^\intercal(\boldsymbol{x}_\Gamma) \end{bmatrix} = \begin{bmatrix} \partial^\Gamma_x u & \partial^\Gamma_y u & \partial^\Gamma_z u \\ \partial^\Gamma_x v & \partial^\Gamma_y v & \partial^\Gamma_z v \\ \partial^\Gamma_x w & \partial^\Gamma_y w & \partial^\Gamma_z w \end{bmatrix} = \nabla_\Gamma \tilde{\boldsymbol{v}} \cdot \mathbf{P} \tag{4}$$

where $\tilde{\boldsymbol{v}}$ is defined in a similar manner as the scalar function $\tilde{f}$ above. Note that the directional gradient of $\boldsymbol{v}$ is not in the tangent space $T_P\Gamma$, i.e. $\boldsymbol{n}^\intercal_\Gamma \cdot \nabla^{\text{dir}}_\Gamma \boldsymbol{v} \neq \mathbf{0}$. An additional projection with $\mathbf{P}$ onto the tangent space $T_P\Gamma$ of the directional gradient $\nabla^{\text{dir}}_\Gamma$ yields the covariant gradient $\nabla^{\text{cov}}_\Gamma$

$$\nabla^{\text{cov}}_\Gamma \boldsymbol{v} = \mathbf{P} \cdot \nabla^{\text{dir}}_\Gamma \boldsymbol{v} \cdot \mathbf{P} = \mathbf{P} \cdot \nabla^{\text{dir}}_\Gamma \boldsymbol{v} \ , \tag{5}$$

with the important properties $\nabla^{\text{cov}}_\Gamma \boldsymbol{v} = \mathbf{P} \cdot \nabla^{\text{cov}}_\Gamma \boldsymbol{v} \cdot \mathbf{P}$ and $\boldsymbol{n}^\intercal_\Gamma \cdot \nabla^{\text{cov}}_\Gamma \boldsymbol{v} = \nabla^{\text{cov}}_\Gamma \boldsymbol{v} \cdot \boldsymbol{n}_\Gamma = \mathbf{0}$. Furthermore, we also need to introduce the directional derivative $\nabla^{\text{dir}}_{\Gamma_i}$ of 2^{nd}-order tensor functions $\boldsymbol{A} : \Gamma \to \mathbb{R}^{3\times 3}$

$$\nabla^{\text{dir}}_{\Gamma_i} \boldsymbol{A} = \frac{\partial^\Gamma \boldsymbol{A}}{\partial^\Gamma_{x_i}} = \begin{bmatrix} \partial^\Gamma_{x_i} A_{11} & \partial^\Gamma_{x_i} A_{12} & \partial^\Gamma_{x_i} A_{13} \\ \partial^\Gamma_{x_i} A_{21} & \partial^\Gamma_{x_i} A_{22} & \partial^\Gamma_{x_i} A_{23} \\ \partial^\Gamma_{x_i} A_{31} & \partial^\Gamma_{x_i} A_{32} & \partial^\Gamma_{x_i} A_{33} \end{bmatrix} \ . \tag{6}$$

In the following, partial surface derivatives of components of vector or tensor fields are denoted as $u^{\text{dir}}_{,i}$ for directional and $u^{\text{cov}}_{,i}$ for covariant derivatives. The tangential divergence of a vector $\boldsymbol{v}$ is defined as

$$\text{div}_\Gamma \boldsymbol{v} = \text{tr}(\nabla^{\text{dir}}_\Gamma \boldsymbol{v}) = \text{tr}(\nabla^{\text{cov}}_\Gamma \boldsymbol{v}) \tag{7}$$

and for 2^{nd}-order tensor functions $\boldsymbol{A}$

$$\text{div}_\Gamma \boldsymbol{A} = \begin{bmatrix} \text{div}_\Gamma[A_{11},\, A_{12},\, A_{13}] \\ \text{div}_\Gamma[A_{21},\, A_{22},\, A_{23}] \\ \text{div}_\Gamma[A_{31},\, A_{32},\, A_{33}] \end{bmatrix} \tag{8}$$

where, the trace of the surface gradient is invariant of the kind of gradient (directional or covariant), although the components are differ.

Next, 2^{nd}-order derivatives of scalar functions are introduced. The directional 2^{nd}-order derivative of a scalar function $f(\boldsymbol{x}_\Gamma)$ is the tangential Hessian matrix $\mathbf{He}^{\text{dir}}$ and is defined as

$$[\mathbf{He}^{\text{dir}}]_{ij} = \partial^{\Gamma\text{dir}}_{x_j}(\partial^{\Gamma}_{x_i} f) = \partial^{\Gamma\text{dir}}_{x_j x_i} f = f^{\text{dir}}_{,ji} \;, \tag{9}$$

which is in general not symmetric [9], i.e. $f^{\text{dir}}_{,ji} \neq f^{\text{dir}}_{,ij}$. With a projection onto the tangent space $T_P\Gamma$, the covariant Hessian matrix $\mathbf{He}^{\text{cov}} = \mathbf{P} \cdot \mathbf{He}^{\text{dir}}$ is defined, which is symmetric as well known in differential geometry [23].

Finally, the Weingarten mapping $\mathbf{H} = \nabla^{\text{cov}}_\Gamma \boldsymbol{n}_\Gamma$ is introduced as in [16], which is equivalent to the second fundamental form in differential geometry. The Weingarten mapping is symmetric and in the tangent space of $T_P\Gamma$. The non-zero eigenvalues of $\mathbf{H}$ are the principle curvatures $\kappa_{1,2}$ and the mean curvature is defined as $\varkappa = \text{tr}(\mathbf{H})$.

3 KIRCHHOFF-LOVE SHELL EQUATIONS

In this section, the linear Kirchhoff-Love shell theory is formulated in the frame of tangential operators based on a global Cartesian coordinate system. In the following, we restrict ourselves to small deformations, which means that the reference and spacial configuration are indistinguishable crucial for the linearised theory. Furthermore, a linear elastic material, which obeys Hooke's law, is assumed. As usual in the Kirchhoff-Love shell theory, the transverse shear deformations and the change of curvature in the material law may be neglected, which restricts the model to thin shells ($t\kappa_{\max} \ll 1$).

3.1 Kinematics

The domain of the shell Ω with thickness t is defined by

$$\Omega = \left\{ \boldsymbol{x} \in \mathbb{R}^3 : |\zeta| \leq \frac{t}{2} \right\} \tag{10}$$

with ζ being the thickness parameter. The middle surface Γ is defined by $\Gamma := \Omega|_{\zeta=0}$, and a point on the middle surface is denoted as $\boldsymbol{x}_\Gamma$. The displacement field $\boldsymbol{u}_\Omega$ of a point $\boldsymbol{P}(\boldsymbol{x}_\Gamma,\, \zeta)$ in the shell continuum Ω takes the form

$$\boldsymbol{u}_\Omega(\boldsymbol{x}_\Gamma,\, \zeta) = \boldsymbol{u}(\boldsymbol{x}_\Gamma) + \zeta \boldsymbol{w}(\boldsymbol{x}_\Gamma) \tag{11}$$

with $\boldsymbol{u}(\boldsymbol{x}_\Gamma) = [u,\, v,\, w]^\intercal$ being the displacement field of the middle surface and $\boldsymbol{w}(\boldsymbol{x}_\Gamma)$ being the difference vector, as illustrated in Figure 2. With the absence of transverse

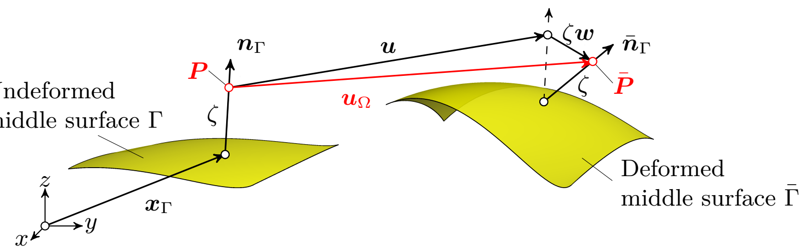

Figure 2: Displacement field $\boldsymbol{u}_\Omega$ of shell continuum

shear deformations, the difference vector $\boldsymbol{w}$ expressed in terms of tangential differential calculus is defined as in [7]

$$\boldsymbol{w}(\boldsymbol{x}_\Gamma) = -\left[\nabla_\Gamma^{\text{dir}}\boldsymbol{u} + (\nabla_\Gamma^{\text{dir}}\boldsymbol{u})^\intercal\right] \cdot \boldsymbol{n}_\Gamma = -\begin{bmatrix} \boldsymbol{u}_{,x}^{\text{dir}} \cdot \boldsymbol{n}_\Gamma \\ \boldsymbol{u}_{,y}^{\text{dir}} \cdot \boldsymbol{n}_\Gamma \\ \boldsymbol{u}_{,z}^{\text{dir}} \cdot \boldsymbol{n}_\Gamma \end{bmatrix} . \tag{12}$$

Consequently, the displacement field of the shell continuum is then only a function of the middle surface displacement $\boldsymbol{u}$, the unit normal vector $\boldsymbol{n}_\Gamma$ and the thickness parameter ζ.

The linearised, in-plane strain tensor $\boldsymbol{\varepsilon}_\Gamma$ is then defined by the projection with $\mathbf{P}$ of the symmetric part of the directional gradient of the displacement field $\boldsymbol{u}_\Omega$ [12]

$$\boldsymbol{\varepsilon}_\Gamma(\boldsymbol{x}_\Gamma, \zeta) = \mathbf{P} \cdot \frac{1}{2}\left[\nabla_\Gamma^{\text{dir}}\boldsymbol{u}_\Omega + (\nabla_\Gamma^{\text{dir}}\boldsymbol{u}_\Omega)^\intercal\right] \cdot \mathbf{P} = \mathbf{P} \cdot \boldsymbol{\varepsilon}_\Gamma^{\text{dir}} \cdot \mathbf{P} \tag{13}$$

where, we have the identity

$$\boldsymbol{\varepsilon}_\Gamma(\boldsymbol{x}_\Gamma, \zeta) = \frac{1}{2}\left[\nabla_\Gamma^{\text{cov}}\boldsymbol{u}_\Omega + (\nabla_\Gamma^{\text{cov}}\boldsymbol{u}_\Omega)^\intercal\right] . \tag{14}$$

Finally, the whole strain tensor may be split into a membrane and bending part, as usual in the classical theory

$$\boldsymbol{\varepsilon}_\Gamma = \boldsymbol{\varepsilon}_{\Gamma,\text{M}}(\boldsymbol{u}) + \zeta\boldsymbol{\varepsilon}_{\Gamma,\text{B}}(\boldsymbol{w}) , \tag{15}$$

with

$$\begin{aligned} [\boldsymbol{\varepsilon}_{\Gamma,\text{M}}]_{ij} &= \frac{1}{2}(u_{i,j}^{\text{cov}} + u_{j,i}^{\text{cov}}) , \\ [\boldsymbol{\varepsilon}_{\Gamma,\text{B}}]_{ij} &= -\boldsymbol{u}_{,ij}^{\text{cov}} \cdot \boldsymbol{n}_\Gamma . \end{aligned}$$

Note that in the linearised bending strain tensor $\boldsymbol{\varepsilon}_{\Gamma,\text{B}}$, the term $(\nabla_\Gamma^{\text{dir}}\boldsymbol{u})^\intercal \cdot \mathbf{H}$ is neglected as in classical theory [21, Remark 2.2] or [24].

3.2 Constitutive Equation

As already mentioned above, the shell obeys Hooke's law and plane stress, which is a suitable assumption for thin structures. Similar to the strain tensor $\boldsymbol{\varepsilon}_\Gamma$ the stress tensor $\boldsymbol{\sigma}_\Gamma$ needs to be in-plane, too [12]

$$\boldsymbol{\sigma}_\Gamma(\boldsymbol{x}_\Gamma, \zeta) = \mathbf{P} \cdot [2\mu\boldsymbol{\varepsilon}_\Gamma + \lambda \mathrm{tr}(\boldsymbol{\varepsilon}_\Gamma)\mathbb{I}] \cdot \mathbf{P} \tag{16}$$

$$= \mathbf{P} \cdot \left[2\mu\boldsymbol{\varepsilon}_\Gamma^{\mathrm{dir}} + \lambda \mathrm{tr}(\boldsymbol{\varepsilon}_\Gamma^{\mathrm{dir}})\mathbb{I}\right] \cdot \mathbf{P} \tag{17}$$

where $\mu = \frac{E}{2(1+\nu)}$ and $\lambda = \frac{E\nu}{(1-\nu^2)}$ are the Lamé constants and $\boldsymbol{\varepsilon}_\Gamma^{\mathrm{dir}}$ is the directional strain tensor from Eq. 13.

3.2.1 Stress resultants

The stress tensor is only a function of the middle surface displacement vector $\boldsymbol{u}$, the difference vector $\boldsymbol{w}$ and the thickness parameter ζ. This enables an analytical pre-integration w.r.t. the thickness and stress resultants can be identified. The following quantities are equivalent to the stress resultants in the classical theory [21, 1], but they are expressed in terms of TDC using a global Cartesian coordinate system. Moreover, the stress resultants may be computed only with directional derivatives, see Eq. 17. The moment tensor is defined as

$$\mathbf{m}_\Gamma = \frac{t^3}{12}\boldsymbol{\sigma}_\Gamma(\boldsymbol{\varepsilon}_{\Gamma,\mathrm{B}}) = \mathbf{P} \cdot \mathbf{m}_\Gamma^{\mathrm{dir}} \cdot \mathbf{P} \ , \tag{18}$$

with

$$\mathbf{m}_\Gamma^{\mathrm{dir}} = -D \begin{bmatrix} (\boldsymbol{u}_{,xx}^{\mathrm{dir}} + \nu\boldsymbol{u}_{,yy}^{\mathrm{dir}} + \nu\boldsymbol{u}_{,zz}^{\mathrm{dir}}) \cdot \boldsymbol{n}_\Gamma & \frac{1-\nu}{2}(\boldsymbol{u}_{,yx}^{\mathrm{dir}} + \boldsymbol{u}_{,xy}^{\mathrm{dir}}) \cdot \boldsymbol{n}_\Gamma & \frac{1-\nu}{2}(\boldsymbol{u}_{,zx}^{\mathrm{dir}} + \boldsymbol{u}_{,xz}^{\mathrm{dir}}) \cdot \boldsymbol{n}_\Gamma \\ & (\boldsymbol{u}_{,yy}^{\mathrm{dir}} + \nu\boldsymbol{u}_{,xx}^{\mathrm{dir}} + \nu\boldsymbol{u}_{,zz}^{\mathrm{dir}}) \cdot \boldsymbol{n}_\Gamma & \frac{1-\nu}{2}(\boldsymbol{u}_{,zy}^{\mathrm{dir}} + \boldsymbol{u}_{,yz}^{\mathrm{dir}}) \cdot \boldsymbol{n}_\Gamma \\ \text{sym.} & & (\boldsymbol{u}_{,zz}^{\mathrm{dir}} + \nu\boldsymbol{u}_{,xx}^{\mathrm{dir}} + \nu\boldsymbol{u}_{,yy}^{\mathrm{dir}}) \cdot \boldsymbol{n}_\Gamma \end{bmatrix}$$

where $D = \frac{Et^3}{12(1-\nu^2)}$ is the flexural rigidity of the shell. The two non-zero eigenvalues of $\mathbf{m}_\Gamma$ are the principle bending moments $m_{1,2}$. For the effective normal force tensor $\tilde{\mathbf{n}}_\Gamma$ we have

$$\tilde{\mathbf{n}}_\Gamma = t\boldsymbol{\sigma}_\Gamma(\boldsymbol{\varepsilon}_{\Gamma,\mathrm{M}}) = \mathbf{P} \cdot \mathbf{n}_\Gamma^{\mathrm{dir}} \cdot \mathbf{P} \ , \tag{19}$$

with

$$\mathbf{n}_\Gamma^{\mathrm{dir}} = \frac{Et}{1-\nu^2} \begin{bmatrix} u_{,x}^{\mathrm{dir}} + \nu(v_{,y}^{\mathrm{dir}} + w_{,z}^{\mathrm{dir}}) & \frac{1-\nu}{2}(u_{,y}^{\mathrm{dir}} + v_{,x}^{\mathrm{dir}}) & \frac{1-\nu}{2}(u_{,z}^{\mathrm{dir}} + w_{,x}^{\mathrm{dir}}) \\ & v_{,y}^{\mathrm{dir}} + \nu(u_{,x}^{\mathrm{dir}} + w_{,z}^{\mathrm{dir}}) & \frac{1-\nu}{2}(v_{,z}^{\mathrm{dir}} + w_{,y}^{\mathrm{dir}}) \\ \text{sym} & & w_{,z}^{\mathrm{dir}} + \nu(u_{,x}^{\mathrm{dir}} + v_{,y}^{\mathrm{dir}}) \end{bmatrix} .$$

Similar to the moment tensor, the two non-zero eigenvalues of $\tilde{\mathbf{n}}_\Gamma$ are in agreement with the effective normal force tensor expressed in local coordinates. Note that for curved shells this tensor is *not* the physical normal force tensor. This tensor only appears in the variational formulation, see Section 4. The physical normal force tensor $\mathbf{n}_\Gamma^{\text{real}}$ is defined by

$$\mathbf{n}_\Gamma^{\text{real}} = \tilde{\mathbf{n}}_\Gamma + \mathbf{H} \cdot \mathbf{m}_\Gamma \tag{20}$$

and is in general not symmetric and also has one zero eigenvalue. The occurrence of the zero eigenvalues in $\mathbf{m}_\Gamma$, $\tilde{\mathbf{n}}_\Gamma$ and $\mathbf{n}_\Gamma^{\text{real}}$ is due to fact that these tensors are in-plane tensors, i.e. $\mathbf{m}_\Gamma \cdot \boldsymbol{n}_\Gamma = \boldsymbol{n}_\Gamma^\intercal \cdot \mathbf{m}_\Gamma = \mathbf{0}$. In other words, the normal vector $\boldsymbol{n}_\Gamma$ is the corresponding eigenvector to the zero eigenvalue.

3.3 Equilibrium

Based on the stress resultants above, we obtain the equilibrium for a curved shell in strong form

$$\text{div}_\Gamma \tilde{\mathbf{n}}_\Gamma + \boldsymbol{n}_\Gamma \text{div}_\Gamma(\mathbf{P} \cdot \text{div}_\Gamma \mathbf{m}_\Gamma) + 2\mathbf{H} \cdot \text{div}_\Gamma \mathbf{m}_\Gamma + [\partial x_i^\Gamma \mathbf{H}]_{jk} [\mathbf{m}_\Gamma]_{ki} = -\boldsymbol{f} \ , \tag{21}$$

with $\boldsymbol{f}$ being the load vector per area on the middle surface Γ. With boundary conditions similar to the classical theory, the complete 4^{th}-order BVP in terms of tangential differential calculus using a global Cartesian coordinate system is defined. The obtained equilibrium does not rely on a parametrization of the middle surface and is equivalent to the equations in [1, 24]. From this point of view, the reformulation of the linear Kirchhoff-Love shell equations in terms of TDC is more general than the classical definition based on parametrizations and local coordinates.

The shell equations in strong form are converted to a weak form by multiplying Eq. 21 with a suitable test function $\boldsymbol{v}$ and using integration by parts, leading to the continuous weak form of the equilibrium.

Find $\boldsymbol{u} \in \mathcal{H}^2(\Gamma)^3 : \Gamma \to \mathbb{R}^3$ such that

$$a(\boldsymbol{u},\, \boldsymbol{v}) = \langle \boldsymbol{f},\, \boldsymbol{v} \rangle + \text{B.T.} \quad \forall\, \boldsymbol{v} \in \mathcal{H}_0^2(\Gamma)^3 \ , \tag{22}$$

with

$$\begin{aligned} a(\boldsymbol{u},\, \boldsymbol{v}) &= \int_\Gamma [\nabla_\Gamma^{\text{dir}} \boldsymbol{v}]_{ij} [\tilde{\mathbf{n}}_\Gamma]_{ij} - (\boldsymbol{v}_{,ji} \cdot \boldsymbol{n}_\Gamma) [\mathbf{m}_\Gamma]_{ij} \ \text{d}\Gamma \ , \\ \langle \boldsymbol{f},\, \boldsymbol{v} \rangle &= \int_\Gamma \boldsymbol{f} \cdot \boldsymbol{v} \ \text{d}\Gamma \ . \end{aligned}$$

In the bending part of the bilinear form $a(\boldsymbol{u},\, \boldsymbol{v})$ remain partial 2^{nd}-order surface derivatives which requires that the trial and test functions need to be in the Sobolev space $\mathcal{H}^2(\Gamma)^3$. In the case of simply supported edges, the boundary conditions are

$$\boldsymbol{u}_{|\partial\Gamma_\text{D}} = \mathbf{0} \quad \text{and} \quad m_{\boldsymbol{t}_{\partial\Gamma}} = 0 \ , \tag{23}$$

with $m_{\boldsymbol{t}_{\partial\Gamma}} = (\mathbf{m} \cdot \boldsymbol{n}_{\partial\Gamma}) \cdot \boldsymbol{n}_{\partial\Gamma}$ being the bending moment along the boundary. In the case of clamped edges, the corresponding boundary conditions are

$$\boldsymbol{u}_{|\partial\Gamma_\text{D}} = \mathbf{0} \quad \text{and} \quad \boldsymbol{n}_{\partial\Gamma} \cdot \left[(\nabla_\Gamma^{\text{dir}} \boldsymbol{u})^\intercal \cdot \boldsymbol{n}_\Gamma \right] = 0 \tag{24}$$

In the case of free edges, the effective boundary forces appear similar as in the classical theory. For more information about boundary conditions and effective boundary forces, we refer to [1].

4 IMPLEMENTATIONAL ASPECTS

The continuous weak form is discretized using isogeometric analysis as proposed by Hughes et al. [15]. The NURBS patch defines the middle surface of the shell and elements are defined by the knot spans of the patch.

There is a fixed set of local basis functions $\{N_i^k(\boldsymbol{r})\}$ of order k with $i = 1, \ldots, n_k$ being the number of control points and the nodal displacements $\{\hat{u}_i, \hat{v}_i, \hat{w}_i\}$ stored at the control points i are the degrees of freedom. Using the isoparametric concept, the shape functions $N_i^k(\boldsymbol{r})$ are NURBS of order k. The surface derivatives of the shape functions are computed as in the surface FEM [11, 10] using NURBS instead of Lagrange polynomials as ansatz and test functions.

The resulting element stiffness matrix $\mathbf{K}_{\text{Elem}}$ is a 3×3 block matrix and is divided into a membrane and bending part

$$\mathbf{K}_{\text{Elem}} = \mathbf{K}_{\text{Elem,M}} + \mathbf{K}_{\text{Elem,B}} \ . \tag{25}$$

The membrane part is defined by

$$\mathbf{K}_{\text{Elem,M}} = t \int_\Gamma P_{ik} \cdot [\hat{\mathbf{K}}]_{kj} \ \mathrm{d}\Gamma \tag{26}$$

$$[\hat{\mathbf{K}}]_{kj} = \mu(\delta_{kj} \boldsymbol{N}^{\text{dir}}_{,a} \cdot \boldsymbol{N}^{\text{dir}^\intercal}_{,a} + \boldsymbol{N}^{\text{dir}}_{,j} \cdot \boldsymbol{N}^{\text{dir}^\intercal}_{,k}) + \lambda \boldsymbol{N}^{\text{dir}}_{,k} \cdot \boldsymbol{N}^{\text{dir}^\intercal}_{,j} \ . \tag{27}$$

The matrix $\hat{\mathbf{K}}$ is determined by the directional 1$^{\text{st}}$-order derivatives of the shape functions $\boldsymbol{N}$, where a summation over $a = 1, 2, 3$ has to be performed. One may recognize that the structure of the matrix $\hat{\mathbf{K}}$ is similar as the stiffness matrix of 3D linear elasticity problems. For the bending part we have

$$[\mathbf{K}_{\text{Elem,B}}]_{ij} = D \int_\Gamma n_i n_j \tilde{\mathbf{K}} \ \mathrm{d}\Gamma \tag{28}$$

$$\tilde{\mathbf{K}} = (1-\nu) \boldsymbol{N}^{\text{cov}}_{,ab} \cdot \boldsymbol{N}^{\text{cov}^\intercal}_{,ab} + \nu \boldsymbol{N}^{\text{cov}}_{,cc} \cdot \boldsymbol{N}^{\text{cov}^\intercal}_{,dd} \ . \tag{29}$$

Again a summation over a, b, c, d has to be performed. The first term of $\tilde{\mathbf{K}}$ is the contraction of the covariant Hessian matrix $\mathbf{He}^{\text{cov}}_\Gamma$ and the second term may be identified as the Bi-Laplace operator. Note that for the Bi-Laplace operator also directional derivatives may used, due to fact that the trace of second order derivatives is invariant. This suggests a further rearrangement of the contraction of the covariant Hessian matrix in order to only use directional derivatives, which is preferred from an implementational aspect of view.

When the shell is given through a parametrization, the resulting element stiffness matrix in the classical theory is equivalent to the element stiffness matrix above, but in the classical setting the computation is more cumbersome due to fact that the local basis vectors and the metric tensor in co- and contra-variant form has to be computed.

The boundary conditions are weakly enforced by Lagrange multipliers. The Lagrange multipliers are discretized by the trace of the shape functions of the domain. The usual assembly yields a linear system of equations in the form

$$\begin{bmatrix} \mathbf{K} & \mathbf{C} \\ \mathbf{C}^\intercal & \mathbf{0} \end{bmatrix} \cdot \begin{bmatrix} \underline{\hat{\boldsymbol{u}}} \\ \hat{\boldsymbol{\lambda}} \end{bmatrix} = \begin{bmatrix} \boldsymbol{f} \\ \mathbf{0} \end{bmatrix} , \tag{30}$$

with $[\underline{\hat{\boldsymbol{u}}}, \hat{\boldsymbol{\lambda}}]^\intercal = [\hat{\boldsymbol{u}}, \hat{\boldsymbol{v}}, \hat{\boldsymbol{w}}, \hat{\boldsymbol{\lambda}}]$ being the sought displacements of the control points and Lagrange multipliers. With the nodal shape functions of the Lagrange multipliers $\boldsymbol{N}_\mathrm{L}$, the constraint matrix $\mathbf{C}$ for simply supported edges is defined by

$$\mathbf{C}^\intercal = \int_{\partial\Gamma_\mathrm{D}} \begin{bmatrix} \boldsymbol{N}_\mathrm{L} \cdot \boldsymbol{N}^\intercal & \mathbf{0} & \mathbf{0} \\ \mathbf{0} & \boldsymbol{N}_\mathrm{L} \cdot \boldsymbol{N}^\intercal & \mathbf{0} \\ \mathbf{0} & \mathbf{0} & \boldsymbol{N}_\mathrm{L} \cdot \boldsymbol{N}^\intercal \end{bmatrix} \mathrm{d}\partial\Gamma \tag{31}$$

and for clamped edges

$$\mathbf{C}^\intercal = \int_{\partial\Gamma_\mathrm{D}} \begin{bmatrix} \boldsymbol{N}_\mathrm{L} \cdot \boldsymbol{N}^\intercal & \mathbf{0} & \mathbf{0} \\ \mathbf{0} & \boldsymbol{N}_\mathrm{L} \cdot \boldsymbol{N}^\intercal & \mathbf{0} \\ \mathbf{0} & \mathbf{0} & \boldsymbol{N}_\mathrm{L} \cdot \boldsymbol{N}^\intercal \\ \boldsymbol{N}_\mathrm{L} \cdot (n_x n_{\partial\Gamma_i} \boldsymbol{N}^{\mathrm{dir}^\intercal}_{,i}) & \boldsymbol{N}_\mathrm{L} \cdot (n_y n_{\partial\Gamma_i} \boldsymbol{N}^{\mathrm{dir}^\intercal}_{,i}) & \boldsymbol{N}_\mathrm{L} \cdot (n_z n_{\partial\Gamma_i} \boldsymbol{N}^{\mathrm{dir}^\intercal}_{,i}) \end{bmatrix} \mathrm{d}\partial\Gamma \, . \tag{32}$$

5 NUMERICAL RESULTS

An example, the Scordelis-Lo roof of the shell obstacle course proposed by Belytschko et al. [2] is chosen. For the convergence analyses the problem is computed with uniform meshes of different polynomial orders $p = [2, 3, 4, 5, 6]$ and $h = [2, 4, 8, 16, 32]$ elements per side. As already mentioned the resulting stiffness matrix is equivalent to the stiffness matrix expressed in the classical setting. Therefore, the same convergence properties as shown in [6, 17] are expected. Other examples (e.g., pinched cylinder, pinched hemispherical shell, . . .) have been considered but are omitted here for brevity.

5.1 Scordelis-Lo roof

The Scordelis-Lo roof is a cylindrical shell loaded by gravity, which is supported with two rigid diaphragms at it curved ends, see Figure 3. In Figure 4a, the deformed shell is illustrated. The colours on the surface are the Euclidean norm of the displacement field $\boldsymbol{u}$. In Figure 4b, the convergence to the reference displacement $w_{\mathrm{max,\,ref}}$ is plotted up to a polynomial order of $p = 6$ as function of the element size $\frac{1}{h}$. The results of the convergence analysis are in agreement with the results in e.g. [6, 17].

6 CONCLUSION & OUTLOOK

We have presented a reformulation of the linear Kirchhoff-Love shell theory in terms of the tangential differential calculus (TDC) using a global Cartesian coordinate system. The obtained equations do not hinge on a parametrization of the middle surface of the shell, which might be seen as a generalization of the classical shell equations. Furthermore, the

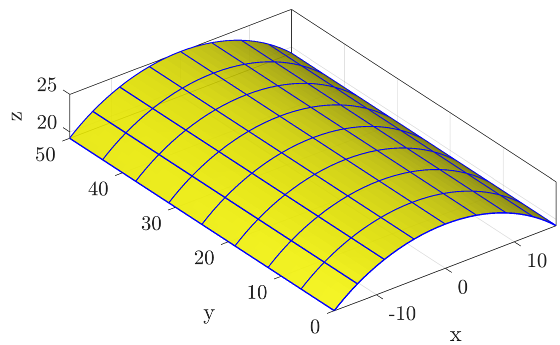

Geometry:	Cylindrical shell $L = 50$ $R = 25$ $\phi = 80°$ $t = 0.25$
Material parameters:	$E = 4.32 \times 10^8$ $\nu = 0.0$
Load:	Gravity load $\boldsymbol{f} = [0,\ 0,\ -90]^\intercal$
Support:	Rigid diaphragms at it curved ends
Reference displacement:	$w_{\text{max, ref}} = 0.3024$

Figure 3: Definition of Scordelis-Lo roof problem [2]

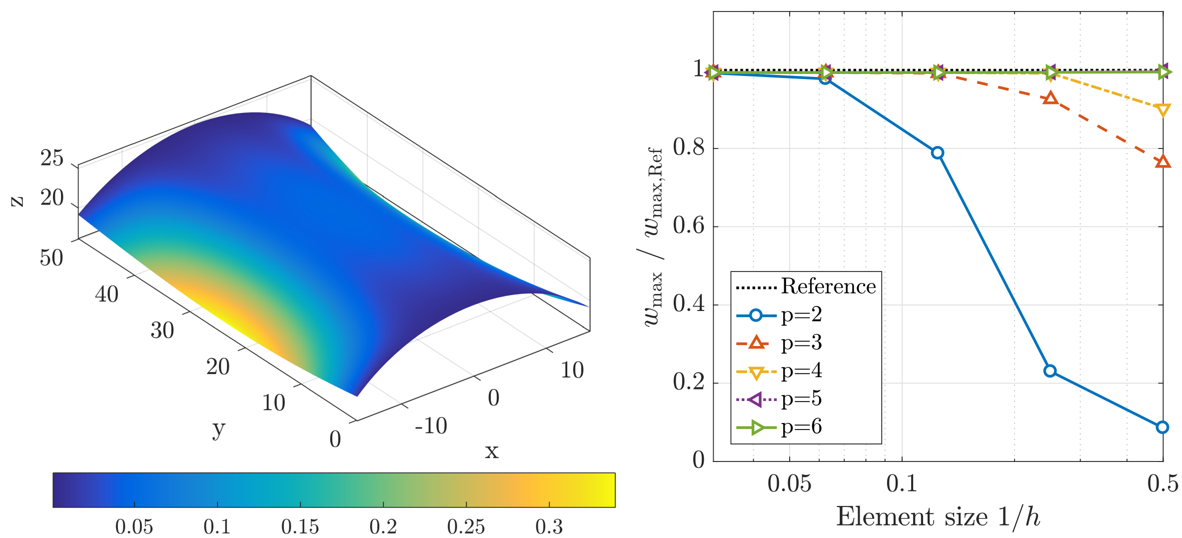

(a) Displacement $\boldsymbol{u}$, exaggerated by one order of magnitude

(b) Normalized convergence of reference displacement $w_{\text{max,Ref}} = 0.3024$

Figure 4: Scordelis-Lo roof

equilibrium in strong form and stress resultants are derived and compared to the classical theory.

For the discretization surface FEM is used with NURBS as trial and test functions. In comparison to the classical theory the reformulation leads to a more compact and intuitive implementation. The numerical results confirm that the proposed formulation is equivalent to the classical formulation and higher-order convergence rates are achieved.

There is a large potential in the reformulation of the shell equations because the obtained PDE may discretized with new finite element techniques such as TraceFEM or CutFEM with implicitly defined surfaces. In our future work, the shell equations are discretized on implicitly defined surfaces without the usage of a parametrization of the middle surface. Furthermore, the Reissner-Mindlin shell equations are recast in terms of TDC.

REFERENCES

[1] Başar, Y.; Krätzig, W.B.: *Mechanik der Flächentragwerke*. Vieweg+Teubner Verlag, Braunschweig, 1985.

[2] Belytschko, T.; Stolarski, H.; Liu, W.K.; Carpenter, N.; Ong, J.S.J: Stress projection for membrane and shear locking in shell finite elements. *Comp. Methods Appl. Mech. Engrg.*, **51**, 221–258, 1985.

[3] Bischoff, M.; Bletzinger, K.U.; Wall, W.A.; Ramm, E.: Models and Finite Elements for Thin-Walled Structures. *Encyclopedia of Computational Mechanics*, John Wiley & Sons, Ltd, Chapter 3, 2004.

[4] Burman, E.; Claus, S.; Hansbo, P.; Larson, M.G.; Massing, A.: CutFEM: Discretizing geometry and partial differential equations. *Internat. J. Numer. Methods Engrg.*, **104**, 472–501, 2015.

[5] Cenanovic, M.; Hansbo, P.; Larson, M.G.: Cut finite element modeling of linear membranes. *Comp. Methods Appl. Mech. Engrg.*, **310**, 98–111, 2016.

[6] Cirak, F.; Ortiz, M.; Schröder, P.: Subdivision surfaces: A new paradigm for thin-shell finite-element analysis. *Internat. J. Numer. Methods Engrg.*, **47**(12), 2039–2072, 2000.

[7] Delfour, M.C.; Zolésio, J.P.: Tangential Differential Equations for Dynamical Thin Shallow Shells. *J. Differential Equations*, **128**, 125–167, 1996.

[8] Delfour, M.C.; Zolésio, J.P.: Differential equations for linear shells comparison between intrinsic and classical. *Advances in Mathematical Sciences: CRM's 25 Years (Montreal, PQ, 1994), CRM Proc. Lecture Notes*, Vol. 11, Providence, Rhode Island, 1997.

[9] Delfour, M.C.; Zolésio, J.P.: *Shapes and Geometries: Metrics, Analysis, Differential Calculus, and Optimization*. Society for Industrial and Applied Mathematics, Philadelphia, 2011.

[10] Demlow, A.: Higher-order finite element methods and pointwise error estimates for elliptic problems on surfaces. *SIAM J. Numer. Anal.*, **47**, 805–827, 2009.

[11] Dziuk, G.; Elliott, C.M.: Finite element methods for surface PDEs. *Acta Numerica*, **22**, 289–396, 2013.

[12] Hansbo, P.; Larson, M.G.: Finite element modeling of a linear membrane shell problem using tangential differential calculus. *Comp. Methods Appl. Mech. Engrg.*, **270**, 1–14, 2014.

[13] Hansbo, P.; Larson, M.G.: Continuous/discontinuous finite element modelling of Kirchhoff plate structures in $\mathbb{R}^3$ using tangential differential calculus. *Comput. Mech.*, **60**, 693–702, 2017.

[14] Hansbo, P.; Larson, M.G.; Larsson, F.: Tangential differential calculus and the finite element modeling of a large deformation elastic membrane problem. *Comput. Mech.*, **56**, 87–95, 2015.

[15] Hughes, T.J.R.; Cottrell, J.A.; Bazilevs, Y.: Isogeometric analysis: CAD, finite elements, NURBS, exact geometry and mesh refinement. *Comp. Methods Appl. Mech. Engrg.*, **194**(39), 4135–4195, 2005.

[16] Jankuhn, T.; Olshanskii, M.A.; Reusken, A.: Incompressible Fluid Problems on Embedded Surfaces Modeling and Variational and Formulations. *ArXiv e-prints*, 2017. ArXiv: 1702.02989.

[17] Kiendl, J.; Bletzinger, K.-U.; Linhard, J.; Wüchner, R.: Isogeometric shell analysis with Kirchhoff–Love elements. *Comp. Methods Appl. Mech. Engrg.*, **198**(49), 3902–3914, 2009.

[18] Lebiedzik, C.: Exact boundary controllability of a shallow intrinsic shell model. *J. Math. Anal. Appl.*, **335**(1), 584–614, 2007.

[19] Reusken, A.: Analysis of trace finite element methods for surface partial differential equations. *IMA J. Numer. Anal.*, **35**, 1568–1590, 2014.

[20] Simo, J.C.; Fox, D.D.: On a stress resultant geometrically exact shell model. Part I: Formulation and optimal parametrization. *Comp. Methods Appl. Mech. Engrg.*, **72**(3), 267–304, 1989.

[21] Simo, J.C.; Fox, D.D.; Rifai, M.S.: On a stress resultant geometrically exact shell model. Part II: The linear theory; Computational aspects. *Comp. Methods Appl. Mech. Engrg.*, **73**(1), 53–92, 1989.

[22] van Opstal, T.M.; van Brummelen, E.H.; van Zwieten, G.J.: A finite-element/boundary-element method for three-dimensional, large-displacement fluid–structure-interaction. *Computer Methods in Applied Mechanics and Engineering*, **284**, 637–663, 2015.

[23] Walker, S.W.: *The Shapes of Things: A Practical Guide to Differential Geometry and the Shape Derivative.* Advances in Design and Control. SIAM, 2015.

[24] Wempner, G.; Talaslidis, D.: *Mechanics of Solids and Shells: Theories and Approximations.* CRC Press LLC, Boca Raton, Florida, 2002.